Original Article

Prognostic value and anti-tumor immunity role of *TMED9* in pan-cancer: a bioinformatics study

Haodi Wang[1#], Yue Wang[2#], Pengyu Tan[1], Yichi Liu[1], Sa Zhou[1], Wenjian Ma[1,3]

[1]College of Biotechnology, Tianjin University of Science and Technology, Tianjin, China; [2]College of Future Education, Beijing Normal University at Zhuhai, Zhuhai, China; [3]College of Biological and Chemical Engineering, Qilu Institute of Technology, Jinan, China

Contributions: (I) Conception and design: H Wang, Y Wang; (II) Administrative support: W Ma; (III) Provision of study materials or patients: Y Wang, Y Liu; (IV) Collection and assembly of data: H Wang, P Tan; (V) Data analysis and interpretation: H Wang, S Zhou; (VI) Manuscript writing: All authors; (VII) Final approval of manuscript: All authors.

[#]These authors contributed equally to this work as co-first authors.

Correspondence to: Wenjian Ma, PhD. Professor, College of Biotechnology, Tianjin University of Science and Technology, 29# 13th Ave., Binhai TEDA, Tianjin 300457, China; College of Biological and Chemical Engineering, Qilu Institute of Technology, Jinan, China. Email: ma_wj@tust.edu.cn.

Background: Transmembrane p24 trafficking protein 9 (*TMED9*) belongs to the TMED family, and its overexpression frequently induces cancer. Studies have demonstrated the association between the overexpression of *TMED9* and cancer development and proliferative migration in cancers such as ovarian cancer, hepatocellular carcinoma, and breast cancer. However, there has been no study investigating the clinical value, biological function, and anti-tumor immune effects of *TMED9* from a pan-cancer perspective. The aim of this study is to evaluate the prognostic value and anti-tumor immunity role of *TMED9* across pan-cancers.

Methods: We utilized R language along with The Cancer Genome Atlas (TCGA), UCSC Xena (University of California, Santa Cruz Xena Browser), Human Protein Atlas (HPA), and other datasets to investigate *TMED9* expression in various tumors. The association between high *TMED9* expression and clinical prognosis and patient survival was examined using the Kaplan-Meier method, log-rank test, as well as univariate and multivariate Cox regression analyses. Tumor Immune Estimation Resource 2.0 (TIMER2.0) and various algorithms were employed to explore the relationship between *TMED9* and the tumor microenvironment (TME). Additionally, the biological function of *TMED9* in cancer was investigated through Gene Ontology (GO), Kyoto Encyclopedia of Genes and Genomes (KEGG), and gene set enrichment analysis (GSEA) analyses.

Results: *TMED9* was over-expressed in the majority of cancers. Patients exhibiting elevated *TMED9* expression typically experienced diminished survival rates and unfavorable clinical outcomes. *TMED9* played a role as a mediator in the aggressive phenotype of numerous tumors, actively engaging in various biological and signaling pathways linked to cancer development. *TMED9* demonstrated the capacity to modulate the anti-tumor immune response in pan-cancer patients, exerting its influence on the infiltration levels of immune cells and cancer-associated fibroblasts (CAFs).

Conclusions: *TMED9* serves as a novel "cancer indicator" and "clinical prognostic marker", capable of reshaping the TME, impacting the immunotherapeutic response, and guiding precise treatments for cancers to a certain extent.

Keywords: Transmembrane p24 trafficking protein 9 (*TMED9*); pan-cancer analysis; prognosis biomarker; tumor microenvironment (TME); cancer immunity

Submitted Feb 17, 2024. Accepted for publication Jul 07, 2024. Published online Sep 11, 2024.
doi: 10.21037/tcr-24-258
View this article at: https://dx.doi.org/10.21037/tcr-24-258

Introduction

Transmembrane p24 trafficking protein (TMED) family comprises type I single-channel transmembrane proteins found in all eukaryotic organisms. Members of this family serve as crucial regulators of protein translocation, influencing the composition, structure, and function of various organelles, particularly the endoplasmic reticulum and Golgi apparatus (1). As a member of the *TMED* family, *TMED9* is involved in transporting, modifying, and packaging proteins or lipids into vesicles, delivering them to specific locations (2).

TMED9 was found to be implicated in the development of various cancers. *TMED9* expression is upregulated in epithelial ovarian cancer compared to normal ovarian epithelium, showing independent prognostic significance for both disease-free survival (DFS) and overall survival (OS) (3). Over-expression of *TMED9* promotes breast cancer cell proliferation and migration, serving as a potential prognostic biomarker and drug target (4). *TMED9* has also been considered a poor prognostic and prognostic predictive biomarker for hepatocellular carcinoma patients (5). Over-expression of *TMED9* promotes colon cancer metastasis by activating the CNIH4/TGFα/GLI signaling pathway (6).

However, no study has comprehensively and meticulously explored the clinical value, biological function, and its role in anti-tumor immunity of *TMED9* in patients with different tumors from a pan-cancer perspective. In this study, we conducted a multidimensional analysis of *TMED9* expression and its potential clinical value in pan-cancer using a bioinformatics approach with R language and various databases, including Tumor Immune Estimation Resource 2.0 (TIMER2.0; http://timer.cistrome.org/), The Cancer Genome Atlas (TCGA; https://portal.gdc.cancer.gov/), Genotype-Tissue Expression (GTEx; https://xenabrowser.net/), The University of Alabama at Birmingham CANcer data analysis portal (UALCAN; https://ualcan.path.uab.edu/), Human Protein Atlas (HPA; https://proteinatlas.org), and Gene Expression Profiling Interactive Analysis 2 (GEPIA2; http://gepia2.cancer-pku.cn/#index). Additionally, we investigated the relationship between *TMED9* expression and anti-tumor immunity in patients with different cancers. Through a series of correlation and expression analyses, we identified the top 100 differentially co-expressed genes with the strongest correlation with *TMED9* expression in 33 different cancers. We further explored the specific biological pathways and signaling pathways associated with cancer development of those genes. We propose that *TMED9* is a novel "cancer indicator" and "clinical prognostic diagnostic marker" capable of remodeling the tumor microenvironment (TME), influencing the immunotherapeutic response, and guiding the precision treatment of various cancers. We present this article in accordance with the TRIPOD reporting checklist (available at https://tcr.amegroups.com/article/view/10.21037/tcr-24-258/rc).

Highlight box

Key findings

- Transmembrane p24 trafficking protein 9 (*TMED9*) is over-expressed in the majority of cancers.
- *TMED9* demonstrates promising clinical prognostic value and holds potential as a diagnostic marker for cancer.
- *TMED9* participates in numerous biological pathways implicated in cancer initiation, development, proliferation, and invasion.
- The expression of *TMED9* correlates with the infiltration levels of cancer-associated fibroblasts and immune cells, suggesting its potential involvement in shaping the tumor microenvironment.

What is known and what is new?

- Studies have demonstrated the association between the overexpression of *TMED9* and cancer development and proliferative migration in cancers such as ovarian cancer, hepatocellular carcinoma, and breast cancer.
- This study comprehensively and meticulously investigates the expression, biological function, mechanisms of cancer involvement, and immune regulation of *TMED9* in various tumors, examining them from multiple perspectives and aspects.

What is the implication, and what should change now?

- *TMED9* emerges as a potential diagnostic and prognostic marker for various tumors, offering a crucial theoretical foundation for personalized cancer treatment and the advancement of novel targeted drugs and immunotherapy targets.

Methods

Data collection and preprocessing

We obtained the differential expression of the *TMED9* gene between tumor tissues and adjacent normal tissues in all TCGA tumor types using TIMER2.0 (7). Utilizing pan-cancer data from the TCGA database (8), we obtained RNA-sequencing data and processed them uniformly by the Toil process (9). The gene expression levels were shown using a $\log_2$(TPM +1) scale, where TPM stands for transcripts per million. The dataset included raw data of *TMED9* (ENSG00000184840.11) expression in 727 paracancerous

normal tissue samples and 9,807 tumor tissue samples. The data underwent $\log_2$(TPM +1) normalization and harmonization based on pan-cancer information from the GTEx dataset, incorporating raw *TMED9* expression data from 7,568 paracancerous normal tissue samples. Employing the HPA database (10), we compiled and acquired *TMED9* messenger RNA (mRNA) expression data from various normal tissues. This study was conducted in accordance with the Declaration of Helsinki (as revised in 2013).

Expression level of TMED9 in pan-cancer patients

We utilized the "Gene DE" module in TIMER2.0 to acquire the differential expression of the *TMED9* gene in all TCGA tumors. We utilized the "limma" R package to obtain the expression data of *TMED9* in both TCGA and GTEx. We employed the "ggplot2" package to visualize the data and create box plots for a visual comparison of the differences in *TMED9* expression between the 33 tumor tissues and normal tissues.

We retrieved immunohistochemical images depicting the differential expression of *TMED9* in tumor tissues and normal tissues across nine cancers: breast invasive carcinoma (BRCA), lung adenocarcinoma (LUAD), lung squamous cell carcinoma (LUSC), stomach adenocarcinoma (STAD), colon adenocarcinoma (COAD), head and neck squamous cell carcinoma (HNSC), kidney renal clear cell carcinoma (KIRC), prostate adenocarcinoma (PRAD), and uterine corpus endometrial carcinoma (UCEC), using the HPA database. Simultaneously, we presented box plots depicting *TMED9* protein expression in these tumor tissues and normal tissues to enhance result validation.

Clinical prognostic value of TMED9 in pan-cancer

The impact of *TMED9* expression on the prognostic value of patients with 33 tumors in TCGA, encompassing OS and DFS, was assessed using GEPIA2 (11). Subsequently, we classified these tumor patients into *TMED9* high-expression (top 50%) and low-expression (bottom 50%) groups based on the median value of *TMED9* expression. We compared the progression-free interval (PFI) between *TMED9* high- and low-expression groups using Kaplan-Meier curves (http://kmplot.com/analysis/) (12) and multifactorial Cox regression. Proportional risk hypothesis testing and fitted survival regressions were conducted using the "survival" package in R. The survival curves were plotted using the "survminer" package. Receiver operating characteristic (ROC) analysis was executed employing the "pROC" package.

We categorized BRCA patients based on race and age, HNSC patients based on N stage, histologic grade, and disease-specific survival (DSS) event, liver hepatocellular carcinoma (LIHC) patients based on race, histologic grade, weight, height, and alpha-fetoprotein concentration, KIRC patients based on histologic grade, DSS event, pathologic stage, and PFI event, LUAD patients based on N stage, smoker, and OS event, and thyroid carcinoma (THCA) patients based on N stage, T stage, and extra-thyroidal invasion. The "stats" and "car" packages in R software were employed for statistical analysis. Visualization was done using the "ggplot2" package. To assess the prognostic potential of *TMED9* in BRCA, HNSC, LIHC, KIRC, LUAD, and THCA, following the methodology outlined by Zhang *et al.* (13), we conducted both univariate and multivariate Cox regression analyses for OS. It is important to note that samples were included in the multivariate Cox model only if they met the set P value threshold ($P<0.1$) in the univariate Cox analysis. Proportional risk hypothesis testing and Cox regression analysis were conducted using the "survival" and "rms" packages in R software.

Role of TMED9 expression in pan-cancer in regulating immune infiltrating cells

Utilizing TIMER2.0, we examined the correlation between *TMED9* expression in various TCGA tumors and diverse immune cells, such as B cells, macrophages, $CD8^+$ T cells, regulatory T cells, cancer-associated fibroblasts (CAFs), $CD4^+$ T cells, myeloid dendritic cells, mast cells, natural killer (NK) cells, neutrophils, and monocytes. We employed multiple algorithms, including TIMER, Estimating the Proportion of Immune and Cancer cells (EPIC), Quantification of Tumor Infiltrating Immune Cells (QUANTISEQ), Xenobiotic Chemical-Responsive Expression Loci (XCELL), Microenvironment Cell Populations-counter (MCPCOUNTER), Cell-type Identification By Estimating Relative Subsets Of RNA Transcripts (CIBERSORT), CIBERSORT Absolute mode (CIBERSORT-abs), and Tumor Immune Dysfunction and Exclusion (TIDE).

Functional enrichment analysis of TMED9 and its differential co-expressed genes in pan-cancer

We obtained the top 100 differential expression genes (DEGs) most similar to *TMED9* from all TCGA tumors

and normal tissues using GEPIA2. Subsequently, we conducted paired gene-gene Pearson correlation analyses between *TMED9* and its DEGs. We employed the "org.Hs.eg.db" package in R V4.2.1 for the ID conversion of DEGs. Additionally, the "clusterProfiler" and "enrichplot" packages were used for Gene Ontology (GO) and Kyoto Encyclopedia of Genes and Genomes (KEGG) enrichment analysis (14). Furthermore, we acquired gene set enrichment analysis (GSEA) gene set [Hallmarks]h.all.v2022.1.Hs.symbols.gmt from the Molecular Signatures Database (MSigDB; https://www.gsea-msigdb.org/gsea/msigdb/collections.jsp) (15) as a reference gene set. We performed GSEA gene enrichment analysis of *TMED9* and its DEGs in six cancers, including BRCA, HNSC, LIHC, KIRC, LUAD, and THCA, using the "ClusterProfiler" and "stringi" R packages. Statistical significance was defined as an adjusted P value <0.05 and false discovery rate (FDR) <0.25, indicating significantly enriched gene sets.

Statistical analysis

All statistical analyses were done using R software (version 4.2.1). We assessed differences in *TMED9* expression between pan-cancerous and normal tissues using the Wilcoxon rank sum test. We evaluated survival differences between *TMED9* high and low expression groups using the Kaplan-Meier method and the log-rank test. We used independent *t*-tests to assess data significance for comparisons between two groups. For comparisons involving more than two groups, we employed the Kruskal-Wallis test. We employed univariate and multivariate Cox analyses to identify potential prognostic factors. We considered statistical significance at P<0.05. Asterisks (*, **, and ***) represent P<0.05, P<0.01, and P<0.001, respectively.

Results

Differential expression analysis of TMED9 in pan-cancer patients

We assessed the expression level of *TMED9* in pan-cancer using TIMER2.0 (*Figure 1A*). *TMED9* expression was significantly upregulated (P<0.001) in various cancers, including bladder urothelial carcinoma (BLCA), BRCA, cholangiocarcinoma (CHOL), COAD, esophageal carcinoma (ESCA), glioblastoma multiforme (GBM), HNSC, KIRC, kidney renal papillary cell carcinoma (KIRP), LIHC, LUAD, LUSC, PRAD, STAD, and UCEC, compared to normal tissues. *TMED9* exhibited high expression in cervical squamous cell carcinoma and endocervical adenocarcinoma (CESC), pancreatic adenocarcinoma (PAAD), pheochromocytoma and paraganglioma (PCPG), and rectum adenocarcinoma (READ); however, the results of the analyses were not discriminatory. In contrast, *TMED9* expression was significantly lower (P<0.001) in THCA tissues compared to normal tissues. Tumor and normal groups are represented by red and blue boxes, respectively.

To address the absence of TCGA normal samples, we gathered uniform TCGA + GTEx data from the UCSC Xena (University of California, Santa Cruz Xena Browser) database. *Figure 1B* illustrates the differential expression of *TMED9* in various tumors, including BLCA, BRCA, CESC, CHOL, COAD, HNSC, KICH, KIRC, LIHC, LUAD, LUSC, PRAD, READ, STAD, and UCEC. These findings align broadly with the results obtained from TIMER2.0. Tumor and normal groups are represented by yellow and blue boxes, respectively. Additionally, we analyzed differences in *TMED9* expression between different tumors and their paired paracancerous normal tissue samples (*Figure 1C*). The results revealed elevated *TMED9* expression in most tumors compared to paired paracancerous normal tissues, and the identified tumor types broadly aligned with the aforementioned analysis. These results suggest that *TMED9* is overexpressed in the majority of cancer types. In addition, using the HPA database we observed that *TMED9* was enriched in the choroid plexus and salivary glands (Figure S1). Various colors denote different organs.

Immunohistochemical analysis of TMED9 in different tumor tissues and normal tissues

To validate the expression of *TMED9* in pan-cancer, differences in *TMED9* mRNA expression and immunohistochemical images in various tumor tissues and normal tissues were verified at the molecular and protein levels, respectively, using UALCAN and HPA databases. Results indicated significant overexpression of *TMED9* in nine cancers, namely BRCA, LUAD, LUSC, STAD, COAD, HNSC, KIRC, and PRAD (P<0.001) (*Figure 2*).

Association of TMED9 with survival in pan-cancer patients

Analyzing the impact of *TMED9* expression on the prognostic OS in 33 different cancers, we generated a heat

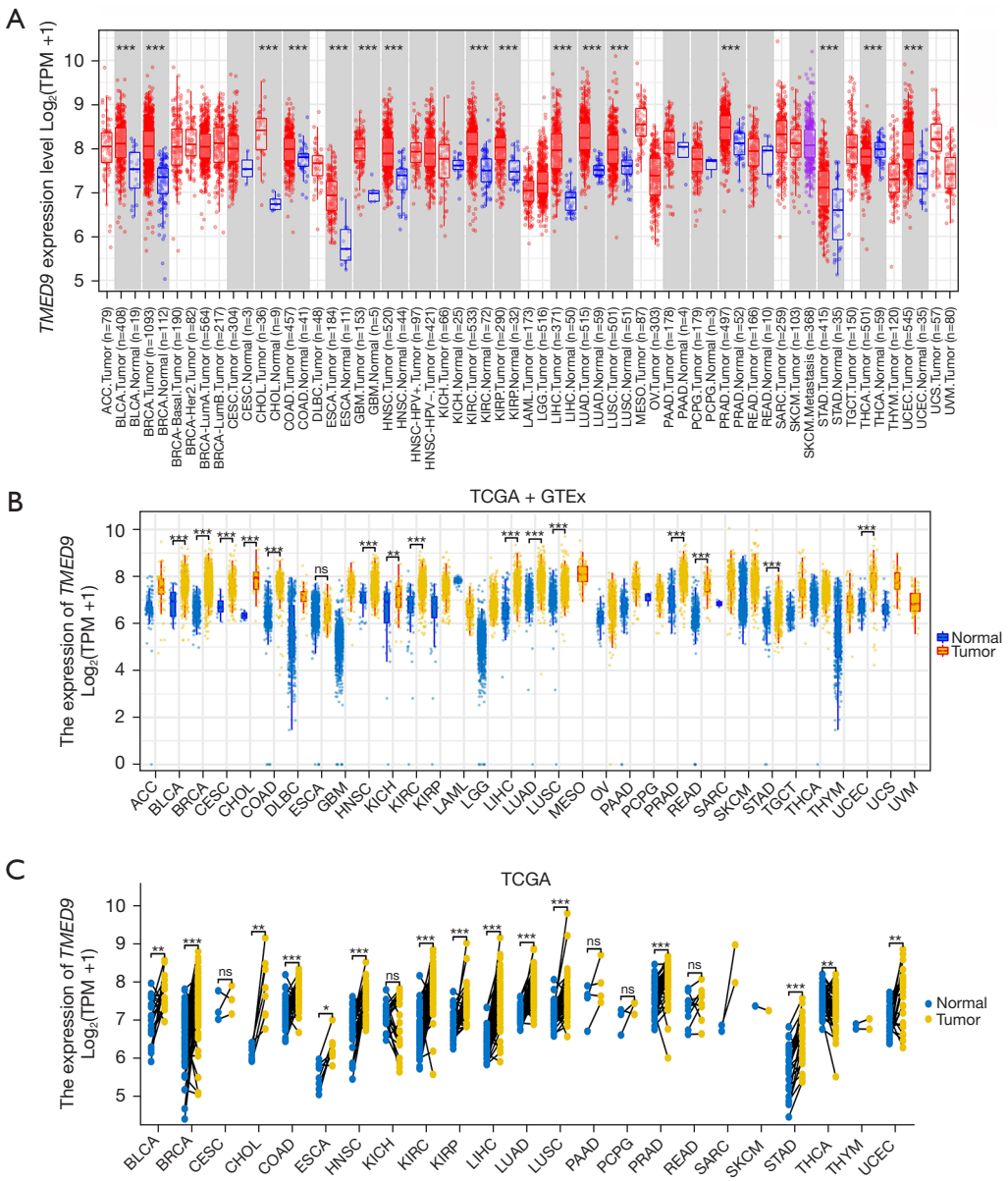

Figure 1 Expression levels of *TMED9* in different tumor tissues and normal tissues. (A) The TIMER2.0 database was utilized to analyze the expression of *TMED9* in various tumors (red) and normal tissues (blue). (B) Analysis of *TMED9* expression in different tumor tissues (yellow) and normal tissues (blue) was conducted using TCGA + GTEx samples. (C) Analysis of *TMED9* expression was conducted in different tumor samples (yellow) and their corresponding adjacent normal paired samples (blue) using TCGA data. ns, P>0.05; *, P<0.05; **, P<0.01; ***, P<0.001. For the full name of the TCGA abbreviations, please see the website: https://gdc.cancer.gov/resources-tcga-users/tcga-code-tables/tcga-study-abbreviations. *TMED9*, transmembrane p24 trafficking protein 9; TPM, transcripts per million; TCGA, The Cancer Genome Atlas; GTEx, Genotype-Tissue Expression; ns, no significance; TIMER2.0, Tumor Immune Estimation Resource 2.0.

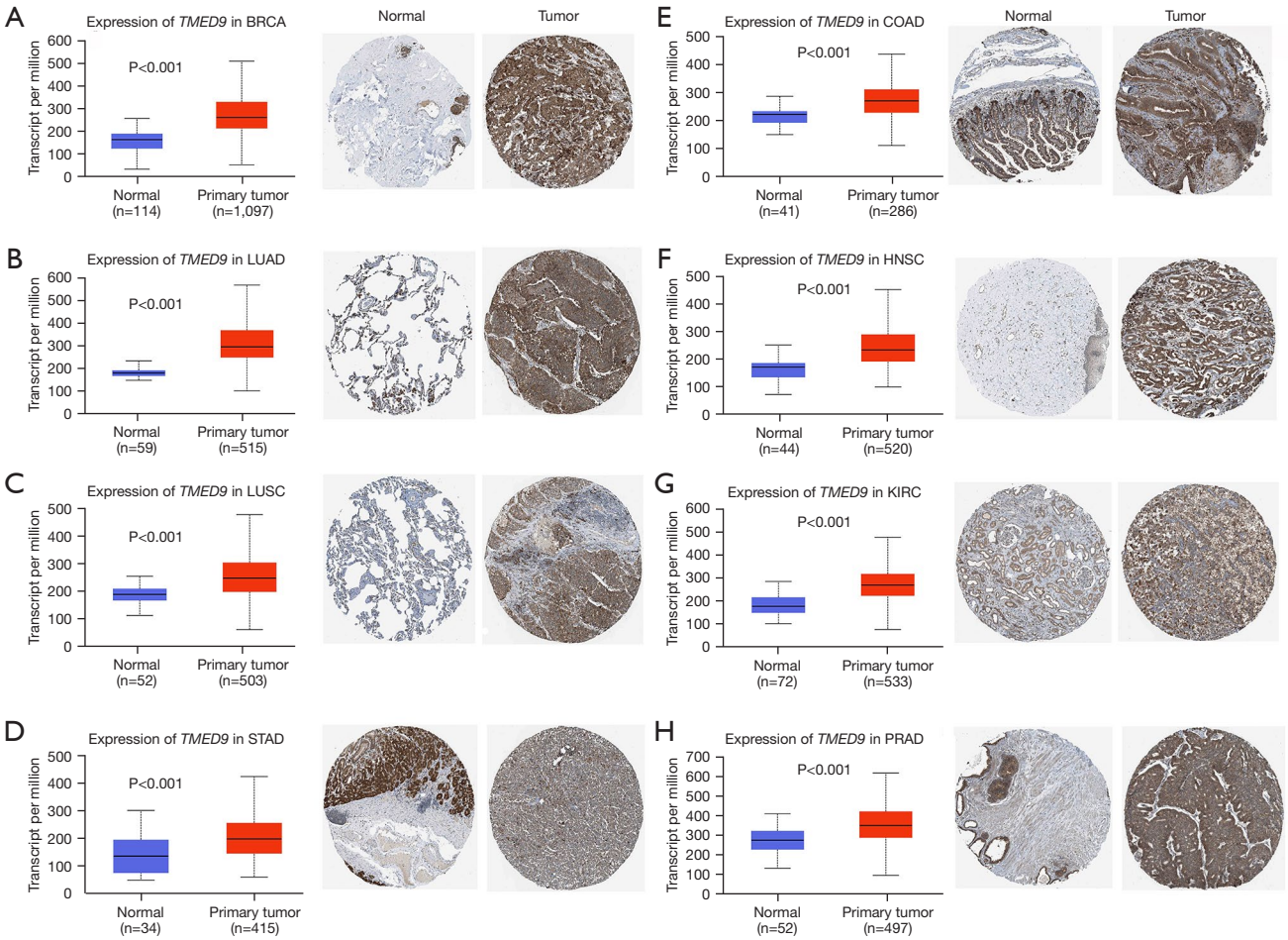

Figure 2 Differential expression of *TMED9* in normal and tumor tissues. *TMED9* mRNA expression and immunohistochemical images in various tumor tissues and normal tissues were validated at the molecular and protein levels, respectively, using UALCAN and HPA databases. HPA images available at https://www.proteinatlas.org/ENSG00000184840-TMED9/pathology. The analyzed tissues include BRCA (A), LUAD (B), LUSC (C), STAD (D), COAD (E), HNSC (F), KIRC (G), and PRAD (H). *TMED9*, transmembrane p24 trafficking protein 9; BRCA, breast invasive carcinoma; LUAD, lung adenocarcinoma; LUSC, lung squamous cell carcinoma; STAD, stomach adenocarcinoma; COAD, colon adenocarcinoma; HNSC, head and neck squamous cell carcinoma; KIRC, kidney renal clear cell carcinoma; PRAD, prostate adenocarcinoma; mRNA, messenger RNA; UALCAN, The University of Alabama at Birmingham CANcer data analysis portal; HPA, Human Protein Atlas.

map. The results revealed a higher correlation between *TMED9* expression and OS in 5 tumors, including BRCA, HNSC, lower-grade glioma (LGG), LIHC, and uveal melanoma (UVM) (*Figure 3A*). Results indicated that high expression of *TMED9* in BRCA (P=0.002), HNSC (P=0.01), LGG (P<0.001), LIHC (P<0.001), and UVM (P=0.006) was associated with poorer OS of patients (*Figure 3B-3F*). Using a similar approach as described above, we investigated the DFS of patients based on *TMED9* expression in cancers. Illustrated in Figure S2A-S2D, high expression of *TMED9* in KIRC (P=0.03), LGG (P<0.001), and mesothelioma (MESO) (P=0.048) was associated with poorer DFS of patients (Figure S2E). Conversely, the low *TMED9* expression group in THCA (P=0.03) exhibited worse DFS. Figure S2F-S2I illustrates TMED9 expression and DFS in patients with CHOL (P=0.10), lymphoid neoplasm diffuse large B-cell lymphoma (DLBC) (P=0.24), KICH (P=0.15), and UVM (P=0.28).

We compared the effects of high and low *TMED9* expression on PFI in cancer patients using Kaplan-Meier

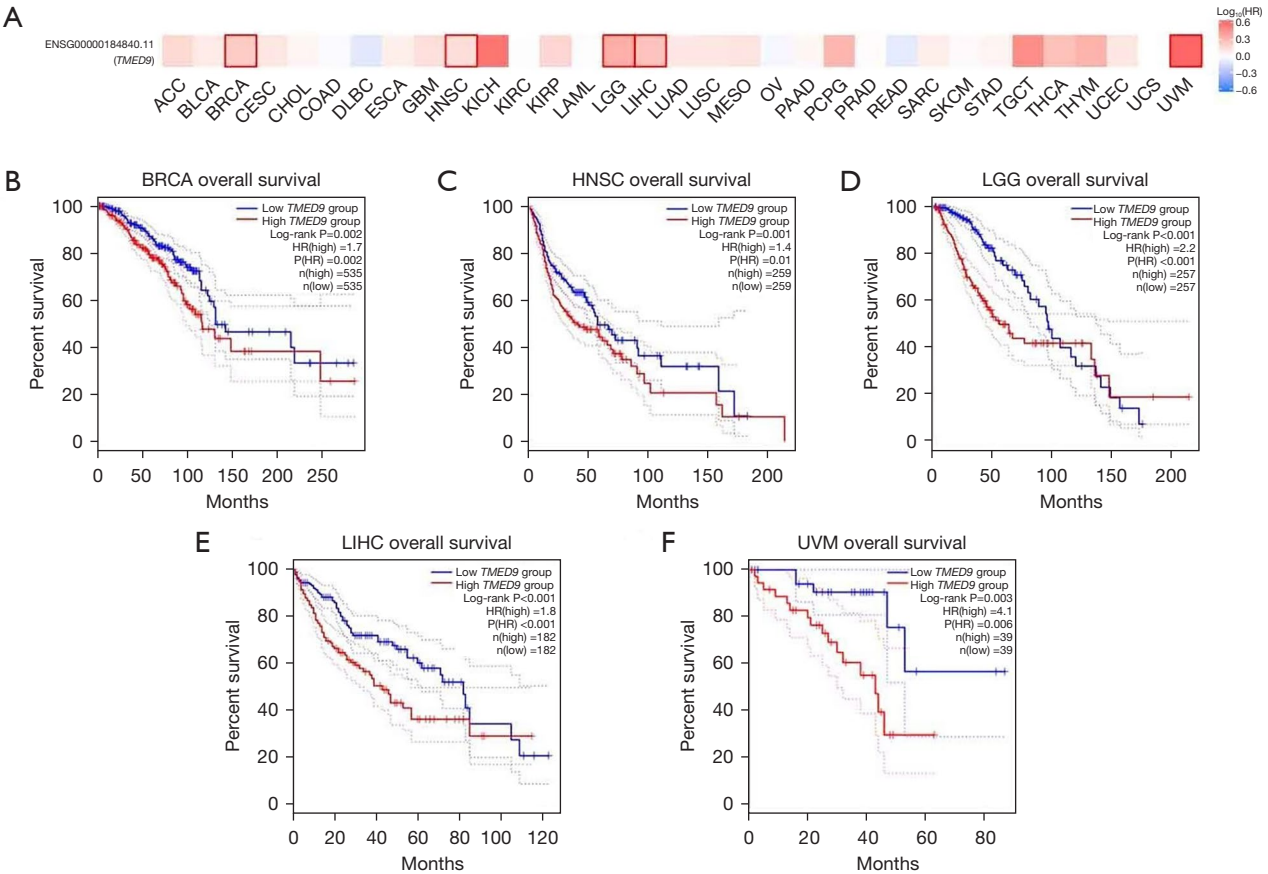

Figure 3 The correlation between *TMED9* expression and OS along with its prognostic significance. (A) The survival map of *TMED9* expression on the OS/prognosis of 33 tumor patients analyzed by GEPIA2. (B-F) Kaplan-Meier plots depicting the correlation between high and low expression levels of *TMED9* in five tumors, namely BRCA, HNSC, LGG, LIHC, and UVM, and the OS of tumor patients. Positive correlations are denoted by red squares, while negative correlations are indicated by blue squares. The red line represents *TMED9* high expression groups, and the blue line represents *TMED9* low expression groups. For the full name of the TCGA abbreviations, please see the website: https://gdc.cancer.gov/resources-tcga-users/tcga-code-tables/tcga-study-abbreviations. *TMED9*, transmembrane p24 trafficking protein 9; HR, hazard ratio; BRCA, breast invasive carcinoma; HNSC, head and neck squamous cell carcinoma; LGG, lower-grade glioma; LIHC, liver hepatocellular carcinoma; UVM, uveal melanoma; OS, overall survival; GEPIA2, Gene Expression Profiling Interactive Analysis 2; TCGA, The Cancer Genome Atlas.

curves and multifactorial Cox regression. As illustrated in Figure S3, high expression of *TMED9* in CESC (P=0.048), HNSC (P=0.001), LGG (P<0.001), COAD (P=0.01), KIRC (P=0.04), and UVM (P=0.04) was associated with poorer PFI in the patients. Conversely, the low *TMED9* expression group in THCA (P=0.007) exhibited worse PFI.

Clinical predictive value of TMED9 in different cancers

We evaluated the clinical diagnostic value of *TMED9* in various cancers by plotting diagnostic ROC curves for *TMED9* expression in patients with BRCA, HNSC, LIHC, KIRC, LUAD, and THCA. The area under the ROC curve values were as follows: 0.880 [95% confidence interval (CI): 0.854–0.906] in BRCA, 0.829 (95% CI: 0.774–0.883) in HNSC, 0.954 (95% CI: 0.930–0.978) in LIHC, 0.841 (95% CI: 0.799–0.882) in KIRC, 0.867 (95% CI: 0.836–0.898) in LUAD, and 0.702 (95% CI: 0.666–0.738) in THCA. These results suggest that *TMED9* expression can distinguish between cancerous and normal tissues in these cancers, indicating clinical diagnostic value (*Figure 4A-4F*).

We investigated the correlation between *TMED9* and

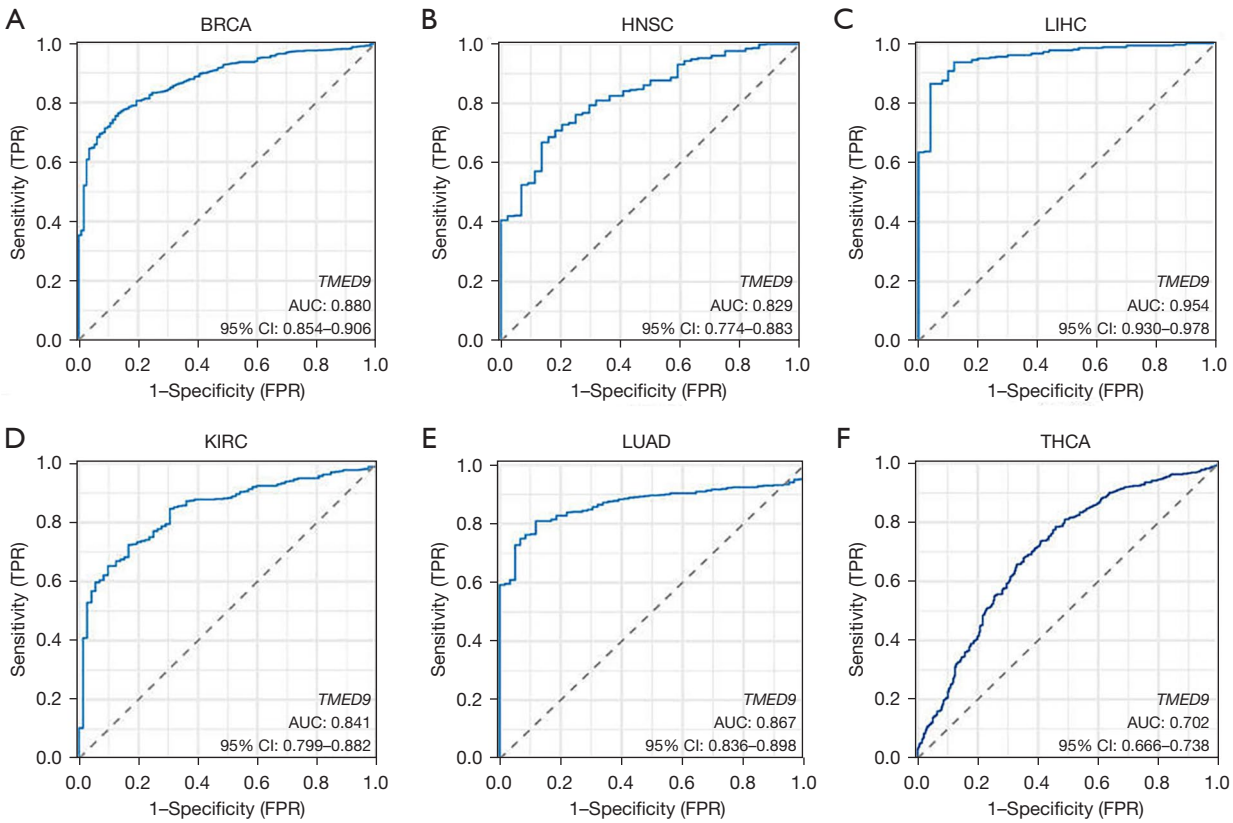

Figure 4 ROC curve analysis demonstrated the robust predictive value of *TMED9* in distinguishing normal tissues from six tumor tissues, namely BRCA (A), HNSC (B), LIHC (C), KIRC (D), LUAD (E), and THCA (F). The AUC is utilized for evaluating prediction accuracy. TPR, true positive rate; FPR, false positive rate; *TMED9*, transmembrane p24 trafficking protein 9; AUC, area under the ROC curve; ROC, receiver operating characteristic; CI, confidence interval; BRCA, breast invasive carcinoma; HNSC, head and neck squamous cell carcinoma; LIHC, liver hepatocellular carcinoma; KIRC, kidney renal clear cell carcinoma; LUAD, lung adenocarcinoma; THCA, thyroid carcinoma.

the clinical characteristics of various cancers. Among BRCA patients, *TMED9* expression was more pronounced in Asians, Blacks, and African Americans compared to Whites (*Figure 5A*). Similarly, among LIHC patients, *TMED9* expression was more pronounced in Asians than in Whites (*Figure 5B*). *TMED9* expression was upregulated with worse tumor N stage in HNSC and LUAD patients (*Figure 5C,5D*). Interestingly, high expression of *TMED9* in THCA was associated with better N0 staging (*Figure 5E*), consistent with the above speculation that *TMED9* may function as a tumor suppressor oncogene in THCA. High expression of *TMED9* in HNSC, LIHC, and KIRC was associated with worse tumor histological grade (*Figure 5F-5H*). High expression of *TMED9* in HNSC and KIRC patients is often associated with death (in DSS event, "yes" indicates that the patient is dead and "no" indicates that the patient is alive) (*Figure 5I,5J*). Additionally, we observed associations between *TMED9* expression and age in BRCA, height, weight, and AFP concentration in LIHC, pathologic stage and PFI event in KIRC, smoker and OS event in LUAD, as well as T-stage and extrathyroidal invasion in THCA (Figure S4). Notably, high expression of *TMED9* in THCA was associated with non-invasive staged tumors (T1 and T2 stages), further confirming our hypothesis that *TMED9* in THCA may act as a suppressor gene.

We conducted univariate and multivariate Cox regression analyses of OS for patients with BRCA, HNSC, LIHC, KIRC, LUAD, and THCA to assess the prognostic utility of *TMED9*. Results showed that high expression of *TMED9* was associated with poorer OS in patients with BRCA, HNSC, LIHC, and LUAD. However, there was no statistically significant association between high *TMED9* expression and poorer OS in KIRC and THCA patients (Tables S1-S6).

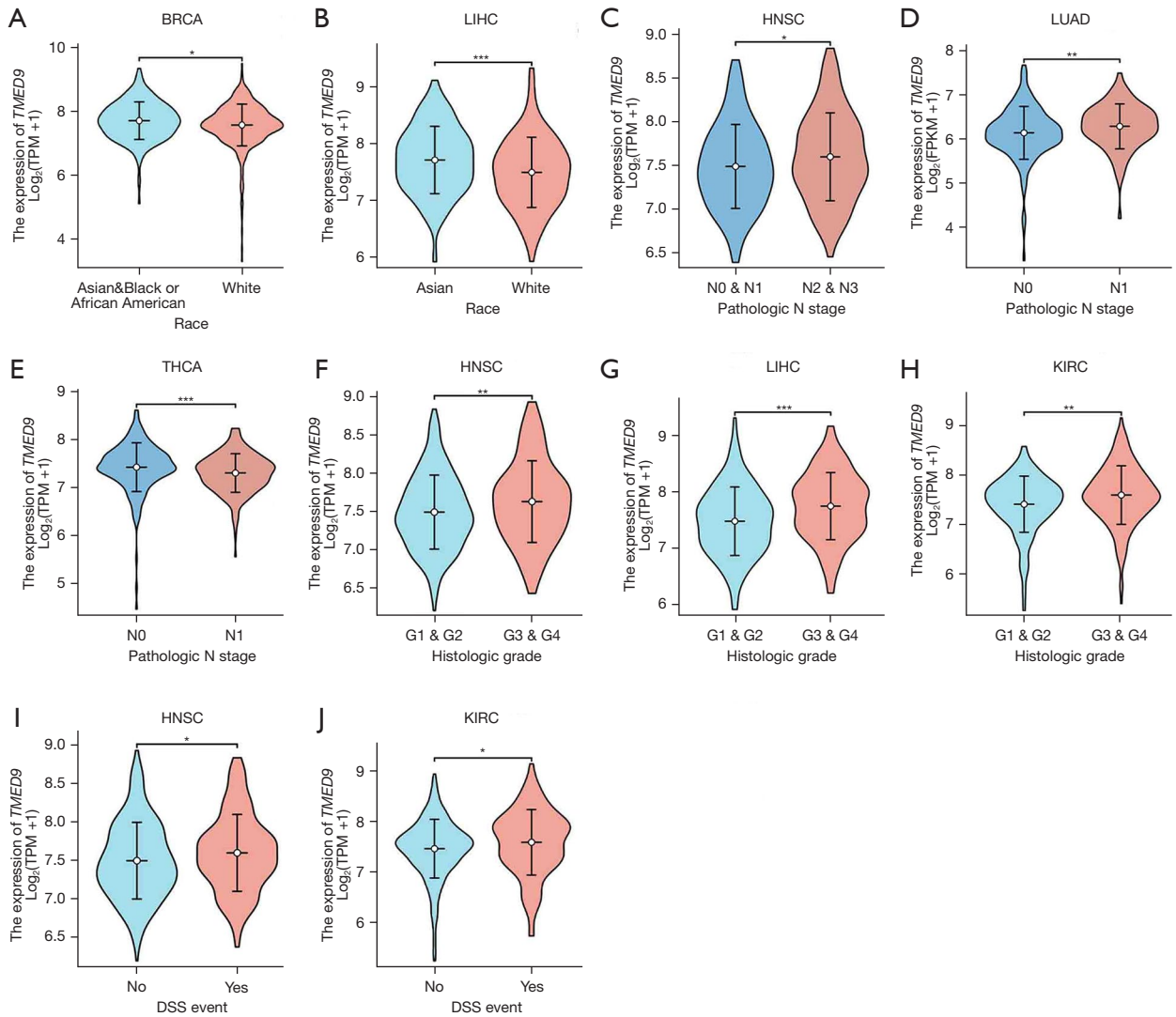

Figure 5 Examining the correlation between *TMED9* expression and diverse clinical parameters in various tumors. *TMED9* expression correlates with race in BRCA (A) and LIHC (B). *TMED9* expression in HNSC (C), LUAD (D), and THCA (E) correlates with N stage representing regional lymph node metastasis. *TMED9* expression correlates with histologic grade in HNSC (F), LIHC (G), and KIRC (H). *TMED9* expression correlates with HNSC (I) and KIRC (J) with DSS event. *, P<0.05; **, P<0.01; ***, P<0.001. *TMED9*, transmembrane p24 trafficking protein 9; TPM, transcripts per million; BRCA, breast invasive carcinoma; LIHC, liver hepatocellular carcinoma; HNSC, head and neck squamous cell carcinoma; LUAD, lung adenocarcinoma; THCA, thyroid carcinoma; KIRC, kidney renal clear cell carcinoma; DSS, disease-specific survival.

Expression of TMED9 in pan-cancer correlates with immune infiltration

We assessed the correlation between *TMED9* expression and the level of immune infiltration in various cancers. Results indicated a positive correlation between *TMED9* expression and B cell infiltration in LIHC (*Figure 6A*) and macrophage infiltration in sarcoma (SARC) (*Figure 6B*). $CD8^+$ T cell infiltration exhibited a negative correlation with *TMED9* expression in PAAD and a positive correlation in UVM (*Figure 6C*). Regulatory T cell exhibited a positive correlation with *TMED9* expression in STAD (*Figure 6D*). However, there was no significant correlation found between *TMED9* expression and infiltration of $CD4^+$ T cell, myeloid dendritic cell, mast cell, NK cell, neutrophil, and

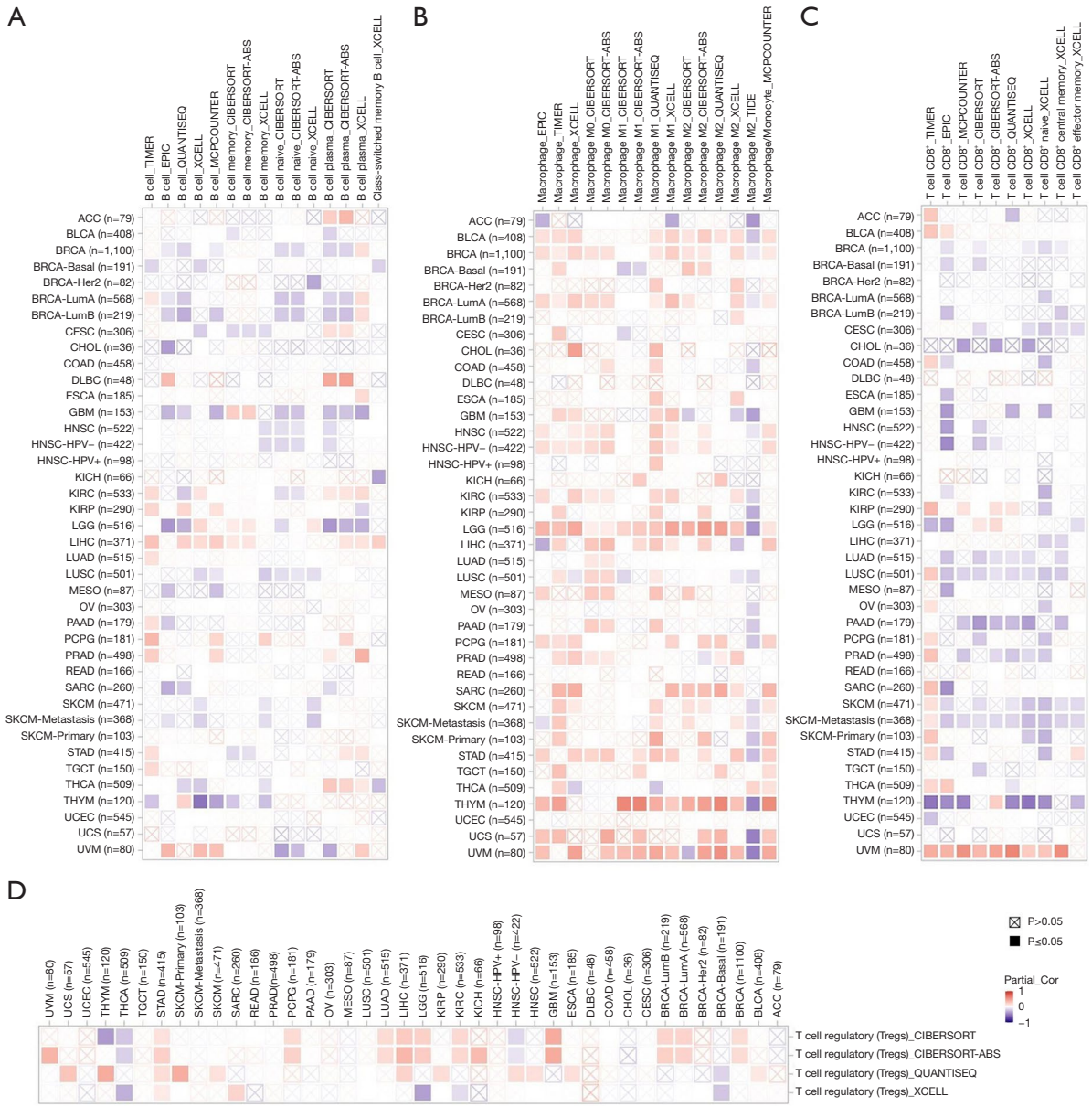

Figure 6 The involvement of *TMED9* in regulating immune infiltrating cells is examined. The association between *TMED9* expression and immune infiltration of B cell (A), macrophage (B), $CD8^+$ T cell (C), and regulatory T cell (D) across pan-cancer is investigated using TIMER2.0. Correlation analysis was conducted utilizing the algorithms TIMER, EPIC, QUANTISEQ, XCELL, MCPCOUNTER, CIBERSORT, CIBERSORT-abs, and TIDE. Positive correlation (0 to 1) is denoted in red, and negative correlation (–1 to 0) is represented in blue. For the full name of the TCGA abbreviations, please see the website: https://gdc.cancer.gov/resources-tcga-users/tcga-code-tables/tcga-study-abbreviations. TIMER, Tumor Immune Estimation Resource; EPIC, Estimating the Proportion of Immune and Cancer cells; QUANTISEQ, Quantification of Tumor Infiltrating Immune Cells; XCELL, Xenobiotic Chemical-Responsive Expression Loci; MCPCOUNTER, Microenvironment Cell Populations-counter; CIBERSORT, Cell-type Identification By Estimating Relative Subsets Of RNA Transcripts; CIBERSORT-abs, CIBERSORT Absolute mode; TIDE, Tumor Immune Dysfunction and Exclusion; Cor, correlation; *TMED9*, transmembrane p24 trafficking protein 9; TCGA, The Cancer Genome Atlas.

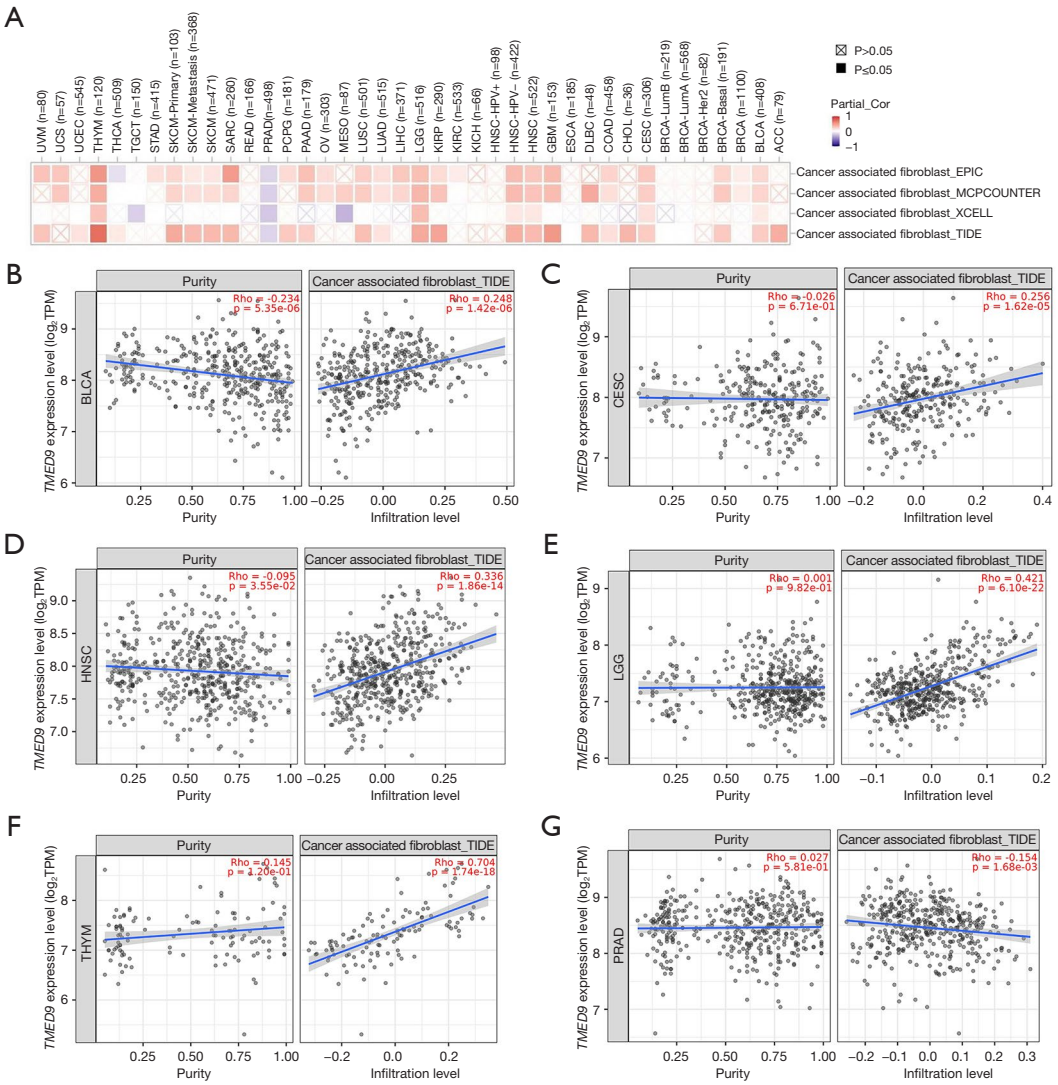

Figure 7 Investigating the correlation between *TMED9* expression and immune infiltration by CAFs. (A-G) Utilizing EPIC, MCPCOUNTER, XCELL, and TIDE algorithms, the correlation between *TMED9* expression and CAFs infiltration was investigated in BLCA, CESC, HNSC, LGG, THYM, and PRAD. For the full name of the TCGA abbreviations, please see the website: https://gdc.cancer.gov/resources-tcga-users/tcga-code-tables/tcga-study-abbreviations. Cor, correlation; EPIC, Estimating the Proportion of Immune and Cancer cells; MCPCOUNTER, Microenvironment Cell Populations-counter; XCELL, Xenobiotic Chemical-Responsive Expression Loci; TIDE, Tumor Immune Dysfunction and Exclusion; *TMED9*, transmembrane p24 trafficking protein 9; TPM, transcripts per million; Rho, Spearman's rank correlation coefficient; BLCA, bladder urothelial carcinoma; CESC, cervical squamous cell carcinoma and endocervical adenocarcinoma; HNSC, head and neck squamous cell carcinoma; LGG, lower-grade glioma; THYM, thymoma; PRAD, prostate adenocarcinoma; CAF, cancer-associated fibroblast; TCGA, The Cancer Genome Atlas.

monocyte in the majority of cancers (Figure S5).

Utilizing EPIC, MCPCOUNTER, XCELL, and TIDE algorithms, we investigated the correlation between CAF infiltration and *TMED9* expression in various malignancies. As depicted in *Figure 7*, *TMED9* expression exhibited a positive correlation with CAF infiltration in patients with BLCA, CESC, HNSC, LGG, and thymoma (THYM), and a negative correlation in patients with PRAD.

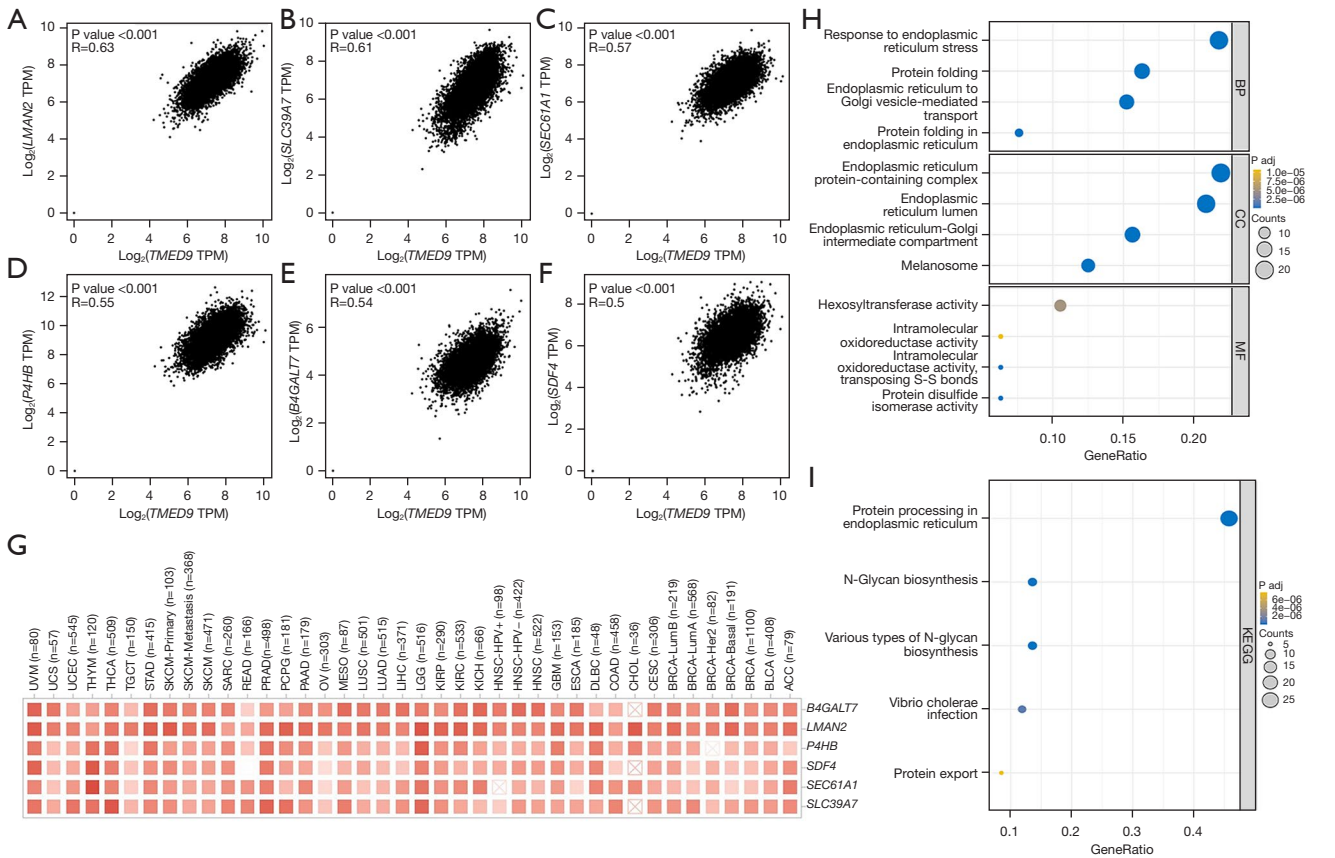

Figure 8 Functional enrichment analysis is performed on the DEGs of *TMED9* in diverse tumors. GEPIA2 revealed a positive association between *TMED9* and six genes: *LMAN2* (A), *SLC39A7* (B), *SEC61A1* (C), *P4HB* (D), *B4GALT7* (E), and *SDF4* (F). (G) The heatmap confirmed a positive correlation between TMED9 expression in pan-cancer tissues and six genes. (H) GO analysis based on 100 *TMED9* DEGs. (I) KEGG pathway enrichment analysis based on 100 *TMED9* DEGs. For the full name of the TCGA abbreviations, please see the website: https://gdc.cancer.gov/resources-tcga-users/tcga-code-tables/tcga-study-abbreviations. *TMED9*, transmembrane p24 trafficking protein 9; TPM, transcripts per million; *LMAN2*, laminin subunit beta-2; *SLC39A7*, solute carrier family 39 member 7; *SEC61A1*, protein transport protein sec61 subunit alpha isoform 1; *P4HB*, beta-subunit of prolyl 4-hydroxylase; *B4GALT7*, beta-1, 4-galactosyltransferase 7; *SDF4*, stromal cell-derived factor 4; BP, biological process; CC, cellular component; MF, molecular function; P adj, adjusted P value; KEGG, Kyoto Encyclopedia of Genes and Genomes; DEG, differentially expressed gene; GEPIA2, Gene Expression Profiling Interactive Analysis 2; GO, Gene Ontology; TCGA, The Cancer Genome Atlas.

Differential gene and its functional enrichment analysis of TMED9

The top 100 DEGs most associated with *TMED9* expression were extracted from all tumor types in the TCGA dataset using GEPIA2; details can be found in Table S7. *Figure 8A-8F* shows that laminin subunit beta-2 (*LAMN2*), solute carrier family 39 member 7 (*SLC39A7*), protein transport protein sec61 subunit alpha isoform 1 (*SEC61A1*), beta-subunit of prolyl 4-hydroxylase (*P4HB*), beta-1, 4-galactosyltransferase 7 (*B4GALT7*), and stromal cell-derived factor 4 (*SDF4*) are highly correlated with *TMED9* expression in most cancer types. Results obtained from using the TIMER2.0 database to verify *TMED9* DEGs were consistent with the above findings (*Figure 8G* and Table S8).

Subsequently, we conducted GO and KEGG analyses on these *TMED9* DEGs. The GO analysis indicated the involvement of these DEGs in biological processes, including mainly response to endoplasmic reticulum stress, protein folding, and endoplasmic reticulum to Golgi vesicle-mediated transport (*Figure 8H*). *Figure 8I* illustrates

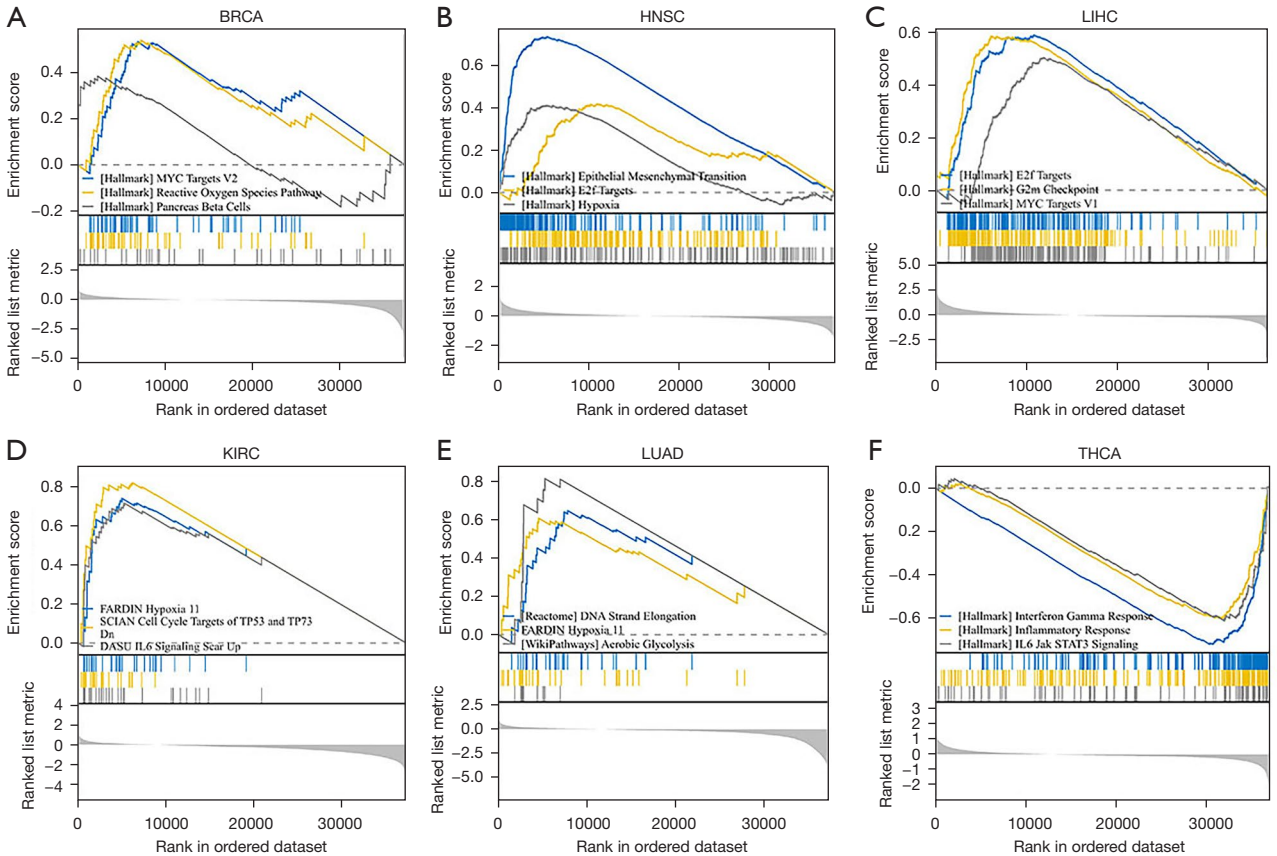

Figure 9 GSEA analysis is conducted to identify cancer-related signaling pathways involving *TMED9*. (A-F) GSEA analysis is conducted on the DEGs of *TMED9* in BRCA, HNSC, LIHC, KIRC, LUAD, and THCA. Various functions or pathways are represented by different colored curves. A peaked curve signifies positive regulation, while a bottomed curve signifies negative regulation of the pathway. BRCA, breast invasive carcinoma; HNSC, head and neck squamous cell carcinoma; LIHC, liver hepatocellular carcinoma; KIRC, kidney renal clear cell carcinoma; LUAD, lung adenocarcinoma; THCA, thyroid carcinoma; GSEA, gene set enrichment analysis; DEG, differentially expressed gene.

the results of KEGG pathway analysis, suggesting the involvement of *TMED9* DEGs in signaling pathways, mainly including protein processing in the endoplasmic reticulum and various types of N-glycan biosynthesis.

We conducted GSEA analysis to explore the biological functions associated with *TMED9* expression in six tumors related to prognosis as illustrated in *Figure 9A*, *TMED9* expression in BRCA was primarily associated with the Myc targets V2 pathway, reactive oxygen species pathway, and pancreas β cells. Within HNSC, *TMED9* was predominantly associated with epithelial-mesenchymal transition (EMT), E2F targeting pathway, and hypoxia (*Figure 9B*). In LIHC, *TMED9* exhibited a primary association with the E2F targeting pathway, G2M checkpoint, and Myc targets V1 pathway (*Figure 9C*). In KIRC, *TMED9* was primarily associated with hypoxia, downregulation of cell cycle targets of *TP53* and *TP73*, and upregulation of the *IL-6* signaling pathway (*Figure 9D*). In LUAD, *TMED9* was predominantly associated with DNA strand elongation, hypoxia, and Aerobic Glycolysis (*Figure 9E*). In THCA, *TMED9* was primarily associated with interferon-gamma (IFN-γ) response, inflammatory response, and the *IL-6-JAK-STAT3* signaling pathway (*Figure 9F*).

Discussion

In this study, we performed a comprehensive pan-cancer analysis to investigate the role of *TMED9* in various cancer types. We observed significant overexpression of *TMED9*

in most of the 33 TCGA cancer types, particularly in BRCA, LUAD, LUSC, STAD, COAD, HNSC, KIRC, and PRAD, compared to normal tissues. Conversely, *TMED9* expression was significantly lower in THCA. Notably, *TMED9* enrichment in the choroid plexus, a crucial hub for immune cell (such as $CCR6^+$ and Th17 cells) entry into brain tissue from the periphery (16), suggests a potential link between *TMED9* expression and the immune system in the context of cancer biology.

Our analysis revealed that high *TMED9* expression was associated with poor OS in BRCA, HNSC, LGG, LIHC, and UVM, poor DFS in KIRC, LGG, and MESO, and poor PFI in CESC, HNSC, LGG, COAD, KIRC, and UVM. Interestingly, low *TMED9* expression in THCA was associated with worse DFS and PFI, suggesting a potential tumor-suppressive role for *TMED9* in this cancer type. ROC curve analysis demonstrated the diagnostic value of *TMED9* expression in distinguishing cancerous tissues from normal tissues in BRCA, HNSC, LIHC, KIRC, LUAD, and THCA. Furthermore, patients with high *TMED9* expression were often associated with poorer clinical parameters, including tumor-node-metastasis (TNM) stage, pathologic stage, histologic grade, R-stage, and advanced malignant phenotypes. These findings strongly indicate that *TMED9* has an oncogenic role in various cancers and is a particularly valuable in predicting prognosis in BRCA, LIHC, HNSC, KIRC, and LUAD.

The TME plays a crucial role in regulating the immune response to tumors, with significant implications for cancer initiation, progression, metabolism, metastasis, and response to therapy (17). Tumor-infiltrating immune cells are crucial components of the TME (18). We observed that highly expressed *TMED9* in many cancers tends to correlate positively with the infiltration degree of immune cells, including B cells, macrophages, $CD8^+$ T cells, and regulatory T cells. Additionally, we found that *TMED9* expression in various malignant tumors correlated with the extent of CAFs infiltration. CAFs are known to regulate various tumor-infiltrating immune cells (19), promote tumor immune evasion (20), metastatic invasion of breast cancers (21), and mediate the proliferation and metastasis of ovarian cancer cells through transactivation of *LINC00092*, a long non-coding RNA involved in increasing glycolysis levels during ovarian cancer metastasis (22). These findings suggest that *TMED9* may influence cancer onset, progression, metastasis, and invasion by modulating the infiltration of various immune cells and CAFs in the TME, highlighting its potential as a key player in cancer immunity and tumor progression.

To further elucidate the functional role of *TMED9* in cancer, we extracted the top 100 DEGs most correlated with *TMED9* expression, and subsequently performed GO and KEGG enrichment analysis. Our results revealed a high correlation between *TMED9* expression and genes such as *LAMN2*, *SLC39A7*, *SEC61A1*, *P4HB*, *B4GALT7*, and *SDF4*. GO analysis suggested that these DEGs may participate in various biological processes and pathways closely linked to tumor development, such as response to endoplasmic reticulum stress, protein folding, endoplasmic reticulum to Golgi vesicle-mediated transport, and protein folding in the endoplasmic reticulum. Endoplasmic reticulum stress plays a crucial role in cancer development and is associated with tumor growth, angiogenesis, metastasis, and chemoresistance (23,24). Aberrant Golgi dynamics can alter the TME and immune landscape, enhancing the invasive and metastatic potential of cancer cells (25,26). KEGG pathway analysis also indicated that *TMED9*-associated DEGs in N-glycan biosynthesis with abnormal N-glycosylation being linked to various aspects of cancer biology, including cell proliferation, migration, and inflammation. Taken together, these findings suggest that the functional expression network of *TMED9* plays a crucial role in tumor proliferation and development.

GSEA analysis revealed that *TMED9* was predominantly involved in various pathways, including Myc targets V1 and V2 pathways, reactive oxygen species pathway, EMT, G2M checkpoint, E2F targets, hypoxia, DNA strand elongation, *IL-6* signaling scar up, *IL-6-JAK-STAT3* signaling pathway, aerobic glycolysis, IFN-γ response, and inflammatory response. The Myc targets VI and V2 pathways are involved in the regulation of cell proliferation and apoptosis, with dysregulation of this pathway leading to carcinogenesis (27). EMT can enhance cancer cell invasion and metastasis by boosting cell motility, extracellular matrix degradation, and immune escape (28,29). The G2M checkpoint pathway is linked to pancreatic cancer cell proliferation and drug response (30). The E2F pathway controls cell proliferation in an oncogenic environment compared to normal cells (31). Reactive oxygen species and hypoxia-induced oxidative stress can activate oncogenic signaling pathways, promote DNA damage, and contribute to tumor development (32). *IL-6* signaling pathway can contribute to tumorigenesis and progression by activating both the *JAK2* and *STAT3* signaling pathways. Aerobic glycolysis promotes cancer cell proliferation, and metastasis by activating oncogenic signaling pathways (33,34). IFN-γ signaling enhances

programmed death-ligand 1 (*PD-L1*) expression, leading to immunosuppression (35). Inflammatory cells and the cytokines they produce are likewise associated with tumor progression. Taken together, we suggest that *TMED9* may influence cancer development by participating in multiple cancer-related pathways.

This study provides strong evidence that *TMED9* is linked to the development and progression of various cancers. However, a limitation of our work is the lack of direct experimental evidence demonstrating how *TMED9* influences cancer-related pathways. In addition, it has been observed that *TMED9* overexpression promotes autophagy, while *TMED9* knockdown diminishes autophagic activity (36,37). Moving forward, we aim to confirm the association of *TMED9* with autophagy in pan-cancer.

Conclusions

In this study, we conclude that *TMED9* serves as a mediator of multiple tumor-invasive phenotypes and is involved in various biological pathways associated with cancer development. *TMED9* may serve as a valid clinical diagnostic marker and an independent prognostic parameter for various cancer types. Additionally, *TMED9* can modulate anti-tumor immune responses in pan-cancer patients by influencing the extent of infiltration of immune cells and CAFs in the TME, along with the expression of various immune checkpoint genes. In conclusion, the present study suggests that *TMED9* is a novel "cancer indicator" and "clinical prognostic marker" that can remodel the TME, influence the immunotherapeutic response, and guide the precision treatment of various cancers to a certain extent.

Acknowledgments

Funding: This work was supported by the National Key R&D Program of China (No. 2018YFA0901702) and the National Science Foundation of Shandong (Nos. ZR2022MC057 and ZR2022MH126).

Footnote

Reporting Checklist: The authors have completed the TRIPOD reporting checklist. Available at https://tcr.amegroups.com/article/view/10.21037/tcr-24-258/rc

Data Sharing Statement: Available at https://tcr.amegroups.com/article/view/10.21037/tcr-24-258/dss

Peer Review File: Available at https://tcr.amegroups.com/article/view/10.21037/tcr-24-258/prf

Conflicts of Interest: All authors have completed the ICMJE uniform disclosure form (available at https://tcr.amegroups.com/article/view/10.21037/tcr-24-258/coif). The authors have no conflicts of interest to declare.

Ethical Statement: The authors are accountable for all aspects of the work in ensuring that questions related to the accuracy or integrity of any part of the work are appropriately investigated and resolved. This study was conducted in accordance with the Declaration of Helsinki (as revised in 2013).

References

1. Zhou L, Li H, Yao H, et al. TMED family genes and their roles in human diseases. Int J Med Sci 2023;20:1732-43.
2. Roberts BS, Satpute-Krishnan P. The many hats of transmembrane emp24 domain protein TMED9 in secretory pathway homeostasis. Front Cell Dev Biol 2023;10:1096899.
3. Han GH, Yun H, Chung JY, et al. TMED9 Expression Level as a Biomarker of Epithelial Ovarian Cancer Progression and Prognosis. Cancer Genomics Proteomics 2022;19:692-702.
4. Ju G, Xu C, Zeng K, et al. High expression of transmembrane P24 trafficking protein 9 predicts poor prognosis in breast carcinoma. Bioengineered 2021;12:8965-79.
5. Yang YC, Chien MH, Lai TC, et al. Proteomics-based identification of TMED9 is linked to vascular invasion and poor prognoses in patients with hepatocellular carcinoma. J Biomed Sci 2021;28:29.
6. Mishra S, Bernal C, Silvano M, et al. The protein secretion modulator TMED9 drives CNIH4/TGFα/GLI signaling opposing TMED3-WNT-TCF to promote colon cancer

metastases. Oncogene 2019;38:5817-37.
7. Li T, Fu J, Zeng Z, et al. TIMER2.0 for analysis of tumor-infiltrating immune cells. Nucleic Acids Res 2020;48:W509-14.
8. Tomczak K, Czerwińska P, Wiznerowicz M. The Cancer Genome Atlas (TCGA): an immeasurable source of knowledge. Contemp Oncol (Pozn) 2015;19:A68-77.
9. Vivian J, Rao AA, Nothaft FA, et al. Toil enables reproducible, open source, big biomedical data analyses. Nat Biotechnol 2017;35:314-6.
10. Navani S. Manual evaluation of tissue microarrays in a high-throughput research project: The contribution of Indian surgical pathology to the Human Protein Atlas (HPA) project. Proteomics 2016;16:1266-70.
11. Tang Z, Kang B, Li C, et al. GEPIA2: an enhanced web server for large-scale expression profiling and interactive analysis. Nucleic Acids Res 2019;47:W556-60.
12. Lánczky A, Győrffy B. Web-Based Survival Analysis Tool Tailored for Medical Research (KMplot): Development and Implementation. J Med Internet Res 2021;23:e27633.
13. Zhang ZF. A comprehensive prognostic and immune infiltration analysis of EXOC3L1 in pan-cancer. Front Genet 2022;13:1044100.
14. Wu T, Hu E, Xu S, et al. clusterProfiler 4.0: A universal enrichment tool for interpreting omics data. Innovation (Camb) 2021;2:100141.
15. Liberzon A, Birger C, Thorvaldsdóttir H, et al. The Molecular Signatures Database (MSigDB) hallmark gene set collection. Cell Syst 2015;1:417-25.
16. Lazarevic I, Soldati S, Mapunda JA, et al. The choroid plexus acts as an immune cell reservoir and brain entry site in experimental autoimmune encephalomyelitis. Fluids Barriers CNS 2023;20:39.
17. Ten A, Kumeiko V, Farniev V, et al. Tumor Microenvironment Modulation by Cancer-Derived Extracellular Vesicles. Cells 2024;13:682.
18. de Visser KE, Joyce JA. The evolving tumor microenvironment: From cancer initiation to metastatic outgrowth. Cancer Cell 2023;41:374-403.
19. Desbois M, Wang Y. Cancer-associated fibroblasts: Key players in shaping the tumor immune microenvironment. Immunol Rev 2021;302:241-58.
20. Gou Z, Li J, Liu J, et al. The hidden messengers: cancer associated fibroblasts-derived exosomal miRNAs as key regulators of cancer malignancy. Front Cell Dev Biol 2024;12:1378302.
21. Ershaid N, Sharon Y, Doron H, et al. NLRP3 inflammasome in fibroblasts links tissue damage with inflammation in breast cancer progression and metastasis. Nat Commun 2019;10:4375.
22. Zhao L, Ji G, Le X, et al. Long Noncoding RNA LINC00092 Acts in Cancer-Associated Fibroblasts to Drive Glycolysis and Progression of Ovarian Cancer. Cancer Res 2017;77:1369-82.
23. Wang R, Huang Y, He J, et al. The endoplasmic reticulum stress-related genes and molecular typing predicts prognosis and reveals characterization of tumor immune microenvironment in lung squamous cell carcinoma. Discov Oncol 2024;15:37.
24. Huang R, Li G, Wang K, et al. Comprehensive Analysis of the Clinical and Biological Significances of Endoplasmic Reticulum Stress in Diffuse Gliomas. Front Cell Dev Biol 2021;9:619396.
25. Bui S, Mejia I, Díaz B, et al. Adaptation of the Golgi Apparatus in Cancer Cell Invasion and Metastasis. Front Cell Dev Biol 2021;9:806482.
26. Bajaj R, Warner AN, Fradette JF, et al. Dance of The Golgi: Understanding Golgi Dynamics in Cancer Metastasis. Cells 2022;11:1484.
27. Ahmadi SE, Rahimi S, Zarandi B, et al. MYC: a multipurpose oncogene with prognostic and therapeutic implications in blood malignancies. J Hematol Oncol 2021;14:121.
28. Datta A, Deng S, Gopal V, et al. Cytoskeletal Dynamics in Epithelial-Mesenchymal Transition: Insights into Therapeutic Targets for Cancer Metastasis. Cancers (Basel) 2021;13:1882.
29. Lai X, Li Q, Wu F, et al. Epithelial-Mesenchymal Transition and Metabolic Switching in Cancer: Lessons From Somatic Cell Reprogramming. Front Cell Dev Biol 2020;8:760.
30. Oshi M, Patel A, Le L, et al. G2M checkpoint pathway alone is associated with drug response and survival among cell proliferation-related pathways in pancreatic cancer. Am J Cancer Res 2021;11:3070-84.
31. Xie D, Pei Q, Li J, et al. Emerging Role of E2F Family in Cancer Stem Cells. Front Oncol 2021;11:723137.
32. Chen PS, Chiu WT, Hsu PL, et al. Pathophysiological implications of hypoxia in human diseases. J Biomed Sci 2020;27:63.
33. Chelakkot C, Chelakkot VS, Shin Y, et al. Modulating Glycolysis to Improve Cancer Therapy. Int J Mol Sci 2023;24:2606.
34. Hosios AM, Manning BD. Cancer Signaling Drives Cancer Metabolism: AKT and the Warburg Effect. Cancer Res 2021;81:4896-8.

35. Singh S, Kumar S, Srivastava RK, et al. Loss of ELF5-FBXW7 stabilizes IFNGR1 to promote the growth and metastasis of triple-negative breast cancer through interferon-γ signalling. Nat Cell Biol. 2020;22:591-602. Erratum in: Nat Cell Biol 2021;23:1048.
36. Kakuta S, Yamaguchi J, Suzuki C, et al. Small GTPase Rab1B is associated with ATG9A vesicles and regulates autophagosome formation. FASEB J 2017;31:3757-73.
37. Evans AS, Lennemann NJ, Coyne CB. BPIFB3 interacts with ARFGAP1 and TMED9 to regulate non-canonical autophagy and RNA virus infection. J Cell Sci 2021;134:jcs251835.

Cite this article as: Wang H, Wang Y, Tan P, Liu Y, Zhou S, Ma W. Prognostic value and anti-tumor immunity role of *TMED9* in pan-cancer: a bioinformatics study. Transl Cancer Res 2024;13(10):5429-5445. doi: 10.21037/tcr-24-258